IMPACT OF GROUND-LEVEL AVIATION EMISSIONS ON AIR QUALITY IN THE WESTERN UNITED STATES

by

Eric Edward Clark

A thesis

submitted in partial fulfillment

of the requirements for the degree of

Master of Science in Civil Engineering

Boise State University

May 2010

BOISE STATE UNIVERSITY GRADUATE COLLEGE

DEFENSE COMMITTEE AND FINAL READING APPROVALS

of the thesis submitted by

Eric Edward Clark

Thesis Title: Impact of Ground-level Aviation Emissions on Air Quality
                 in the Western United States

Date of Final Oral Examination: 29 August 2008

The following individuals read and discussed the thesis submitted by Eric Edward
Clark, and they evaluated his presentation and response to questions during the final oral
examination. They found that the student passed the final oral examination.

Sondra M. Miller, Ph.D., P.E.   Chair, Supervisory Committee

Molly M. Gribb, Ph.D., P.E.   Member, Supervisory Committee

Amit Jain, Ph.D.   Member, Supervisory Committee

The final reading approval of the thesis was granted by Sondra M. Miller, Ph.D.,
P.E., Chair of the Supervisory Committee. The thesis was approved for the Graduate
College by John R. Pelton, Ph.D., Dean of the Graduate College.

ACKNOWLEDGMENTS

I would like to thank my advisor, Dr. Sondra M. Miller, for her guidance throughout this research project. Also, a special thanks to Dr. Saravanan Arunachalam of the University of North Carolina Chapel Hill (UNC/CH) for his assistance in understanding CMAQ modeling. Thank you to Masters student Mr. Tudor Masek of the Massachusetts Institute of technology (MIT) for helping make this project a success. Also, Dr. Amit Jain was instrumental in helping me configure the Boise State University (BSU) cluster and understanding the basics of Linux; thank you for being part of my committee. Dr. Molly Gribb was also a great help in critiquing this thesis and providing many beneficial suggestions. Finally, I would like to thank both of my parents for their never-ending support and editing of this thesis. Thank you to everyone else who helped me along the way.

ABSTRACT

Impact of Ground-level Aviation Emissions on Air Quality

in the Western United States

Eric Edward Clark

Master of Science in Civil Engineering

The aviation industry has experienced sustained growth since its inception resulting in an increase in air pollutant emissions. Exposure to particulate matter less than 2.5 μm in diameter ($PM_{2.5}$) has been linked to respiratory health problems because it penetrates deepest into human lungs.

This thesis focused on the concentrations of three secondary aerosol species (i.e., sulfate, nitrate + ammonium and organic carbon) as they relate to the formation of total $PM_{2.5}$. There were three goals of this research: evaluate differences in total $PM_{2.5}$ concentration as (1) ground-level aviation emissions (i.e., up to 3,000 ft.) varied, (2) meteorological conditions varied, and (3) the resulting effects on human health.

The Community Multiscale Air Quality (CMAQ) model was used to simulate the effects of increasing or decreasing ground-level aviation emissions from current values. Randomly generated multiplicative factors were applied to current ground-level aviation emissions, resulting in 25 CMAQ simulations representing increases or

decreases in aviation activities. Ground-level aviation emissions were varied and used as inputs to CMAQ.

A sensitivity analysis was performed for these 25 simulations to assess the effects of changes in aviation-associated ground-level emissions and meteorology on total $PM_{2.5}$ concentration. Outputs from these simulations were compared to a base case simulation, which represented current ground-level aviation emissions.

Meteorological variables played a larger role in total $PM_{2.5}$ concentration than variations in ground-level aviation emissions. For example, while holding the other two secondary aerosol emissions at current levels, a 342% increase in sulfate emissions caused a 2.06% increase in sulfate secondary aerosol concentration and a 1.2% increase in total $PM_{2.5}$ concentration over current ground-level aviation activities. In contrast, changes in relative humidity from winter to summer lead to an 18.9% decrease in total $PM_{2.5}$ concentration. The results of these analyses are discussed, while the potential human health effects due to changes in aviation emissions are examined using BenMap.

TABLE OF CONTENTS

LIST OF TABLES

LIST OF FIGURES

CHAPTER 1

INTRODUCTION

1.1   Context

As society advances and the world's population increases, air travel will continue to be a widely used mode of transportation. Reduction in airfare has made flying more economically feasible, translating to more flights both nationally and globally. The average airfare decreased a total of ten dollars in the United States from 1994 to 2004 (Smallen, 2007). The average American family income increased from \$40,611 to \$54,061 annually during that same time (DeNavas-Walt *et al.*, 2005). The number of passengers enplaned on commercial flights for the 40 largest airports increased from 501 million in 1995 to 652 million in 2004, an increase of nearly 30% (DOT, 2007). Although there have been decreases in short-term air traffic due to high fuel costs and increased additional fees, air travel is predicted to double over the next twenty years (ICAO, 2007).

Compounds from the combustion of aircraft fuel include volatile organic compounds ($VOCs$), ozone (O_3), nitrogen oxides (NO_x) and particulate matter (PM). Particulate matter less than 2.5 μm in diameter ($PM_{2.5}$) has been shown to penetrate deepest into the human lungs (Chen *et al.*, 2007). Chronic bronchitis, asthma, and pulmonary edema may develop over time if an individual is exposed to $PM_{2.5}$ concentrations of 20 $\mu g \ m^{-3}$ or higher for five to ten years (Abbey *et al.*, 1995).

Primary and secondary aerosol species comprise total $PM_{2.5}$. Primary aerosols from the exhaust of aircraft engines considered for this study include elemental carbon (EC) and crustal material (CM). Secondary aerosols form within minutes to days in the atmosphere from precursor gases (e.g., sulfur dioxide (SO_2), NO_x, and $VOCs$). These precursor gases form secondary aerosols, such as sulfate (SO_4^{2-}) and nitrate (NO_3^-), primarily through oxidation. Gas-to-particle (gtp) processes allow secondary aerosols to change their size and composition by way of several mechanisms. Gases may condense, coagulate with other particles or transform due to a chemical reaction (Gryning & Chaumerliac, 1997).

For this study, the interaction of primary aerosols (i.e. EC and CM) and three secondary aerosols (i.e., SO_4^{2-}, organic carbon (OC), and semi-volatile PM (ammonium (NH_4^+)+ nitrate (NO_3^-)) in the formation of total $PM_{2.5}$ were considered. These specific aerosols were considered because they are the default components within CMAQ that comprise total $PM_{2.5}$ (Ching & Byun, 1999).

1.2   Scope

The hypothesis of this research was that ground-level aviation emissions have an adverse impact on human health in areas surrounding airports by increasing total $PM_{2.5}$ concentration. The goal of this study was to analyze changes in both ground-level aviation secondary aerosol emissions and meteorology to see which had more of an impact on total $PM_{2.5}$ concentration. Secondary aerosol emissions were varied because they are related to potential future congressional policy changes related to regulating fuel content. The emission increases were then related to human health from a mortality and monetary perspective. The Community Multiscale Air Quality

(CMAQ) model version 4.5 (Ching & Byun, 1999) was used to simulate 25 emissions scenarios. These scenarios were developed by varying secondary aerosol species emissions from a base case simulation representing current ground-level aviation emissions; the output of which were secondary aerosol concentrations summed together with primary aerosols to determine total $PM_{2.5}$ concentration.

The primary and secondary aerosol species with their corresponding CMAQ species are listed in Table 1.1. It should be noted that the I and J in each equation represent Aitken and Accumulation modes. Each mode is defined by the diameter range of a given particle (Aitken: 0.001 to 0.1 μm and Accumulation: 0.1 to 1.0 μm) (Binkowski, 1999). The letter A in the CMAQ Component Species column is the designation for *aerosol*.

Table 1.1: Primary and secondary aerosol species considered in this study.

Species	Parameter Names	CMAQ Component Species
Elemental Carbon (EC)	PM EC	AECI + AECJ
Crustal Material (CM)	PM OTH	A25I + A25J
Sulfate (SO_4^{2-})	PM SULF	ASO4I + ASO4J
Nitrate (NO_3^-)	PM NITR	ANO3I + ANO3J
Ammonium (NH_4^+)	PM AMM	ANH4I + ANH4J
Organic Carbon (OC)	PM OC	AORGAI + AORGAJ + AORGBI + AORGBJ + AORGBJ + 1.167*(AORGPAI + AORGPAJ)

Analyses were performed to determine the impact of each secondary aerosol species on total $PM_{2.5}$ concentration. Similarly, seasonal comparisons were made to assess the impact of meteorological conditions (i.e., temperature, humidity and wind speed). Finally, a U.S. Environmental Protection Agency (U.S. EPA) computer program, BenMap (Hubbell, 2008), was implemented to assess potential future health effects related to changes in total $PM_{2.5}$ concentration for Boise, Idaho.

CHAPTER 2

BACKGROUND

2.1 CMAQ Platform

Beginning in the early 1970s, and through the late 1980s, air quality models were designed for specific pollutants of interest. For example, the Regional Acid Deposition Model was developed for acid rain and the Sulfur Transport and Emissions Model was developed for sulfur (Ching & Byun, 1999). The Community Multiscale Air Quality (CMAQ) model (Ching & Byun, 1999) was developed to incorporate a multitude of air quality issues into one comprehensive model. Although only total $PM_{2.5}$ concentration was examined for this thesis, many more pollutants were simulated for which the data could be analyzed in the future.

CMAQ is a three-dimensional Eulerian modeling system that simulates atmospheric chemistry and contaminant transport (Gillani & Godowitch, 1999). The Eulerian method allows for instantaneous mixing of emissions for each source within a uniform grid. Changes in emissions are computed at each grid cell for multiple species at each time step. The model accounts for emissions, advection, dispersion, chemical formation and meteorology. CMAQ requires gridded meteorological and emissions input data along with initial and boundary conditions to compute each species concentration within the model grid domain. CMAQ can be used to model varying spatial scales, from urban to continental. CMAQ is comprised of several

processors, all of which are controlled by the CMAQ Chemical Transport Model (CCTM). The CCTM simulates all relevant atmospheric chemistry, transport and depositional processes simultaneously so that interaction between each process is simulated accurately (Ching & Byun, 1999).

CMAQ was used to simulate $PM_{2.5}$ concentration response to ground-level aviation emissions across the continental United States. Due to long CMAQ processing times, the 25 model simulations were collaboratively performed at Boise State University (BSU), the University of North Carolina at Chapel Hill (UNC/CH) and the Massachusetts Institute of Technology (MIT).

2.1.1 Geographic Domain

A 36-km grid encompassing the continental United States, portions of Canada, Mexico and the Caribbean was used as the domain for CMAQ simulations. This domain ranged from 24° N to 52° N latitude and 66° W to 126° W longitude and was divided into 148 north-south columns and 112 east-west rows. Data from a subset of the domain (i.e., this study area) were used to perform comparative analyses of changes in total $PM_{2.5}$ concentration related to variations in ground-level aviation activities in specific western United States cities. The subset was derived from a domain for the western United States used by the Western Regional Air Partnership (WRAP) (Tonnesen *et al.*, 2005a). This study area was bounded by the Pacific Ocean to the west and the eastern borders of North and South Dakota to the east. The relative geographic location of the two domains is shown in Figure 2.1.
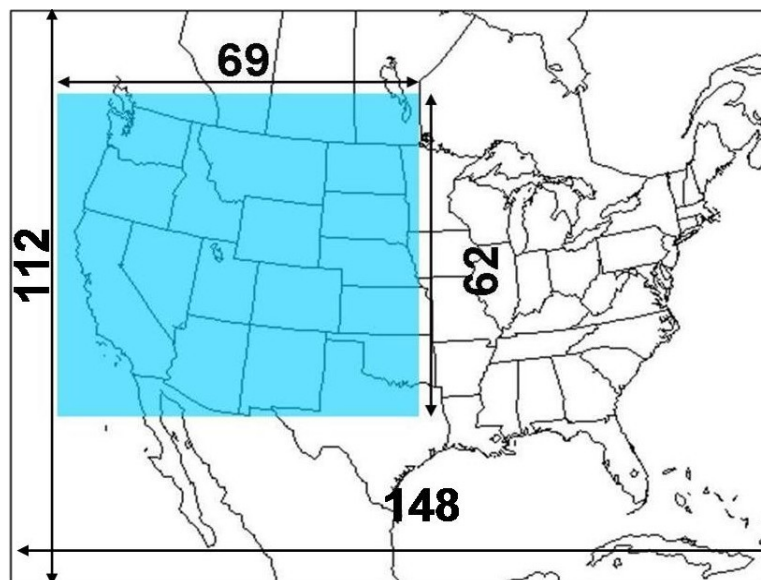
Figure 2.1: The relative geographic location of the two domains. The entire domain (112 by 148, 36-km cells) was used for all the simulations. The subset (62 by 69, 36-km cells) represented the study area for this work: the western United States.

2.1.2 Temporal Allocation

Each of the 25 CMAQ simulations represented one calendar year, divided into four one-month long simulations to reduce computational time. The four simulated months were February, April, July, and October. These months were selected because they represented mean seasonal atmospheric conditions most accurately. Further, these four months matched those previously simulated by the U.S. EPA (EPA, 2006). Each simulation month included a five day spin-up used to bring the initial conditions into equilibrium with the simulated atmospheric state.

2.1.3 Meteorology and Background Emissions

The CMAQ simulations required input of background (e.g., motor vehicle and industrial sources) emissions and meteorological data. Background emissions data

from the National Emissions Inventory (NEI) (EPA, 2007) were used in this study. Ground-level aviation emissions from the NEI were excluded. Instead, the ground-level aviation emissions used for this study were the result of direct measurements at three airports. Meteorological data were simulated using the Mesoscale Model version 5 (MM5) (McNally, 2003). All background emissions and meteorological data were for the year 2001.

2.2   Ground-level Aviation Emissions

Ambient air quality measurements were made at three airports of varying size, traffic and operations. O'Hare International Airport (ORD) in Chicago, Illinois represented the largest cities and airports. William B. Hartsfield Airport (ATL) in Atlanta, Georgia represented medium cities and airports. T.F. Green Airport (PVD) in Providence, Rhode Island represented small cities and airfields. It is important to note that these three airports are located east of the Mississippi River, which may introduce uncertainty due to regional differences. Emissions data for the three airports were computed using the Emissions and Dispersion Modeling System (EDMS) version 5.0.2, which uses a variety of U.S. EPA models and data from the Committee on Aviation Environmental Protection (CAEP) (Thrasher & Soucacos, 2007). Aviation emissions were then processed through the Sparse Matrix Operator Kernel Emissions (SMOKE) version 2.3 prior to running simulations with CMAQ (UNC, 2008). Ground-level aviation emissions inventories included only landing and take-off (i.e., up to 3,000 feet above ground surface). The geographic locations of the 325 airports considered in this study are shown in Figure 2.2.
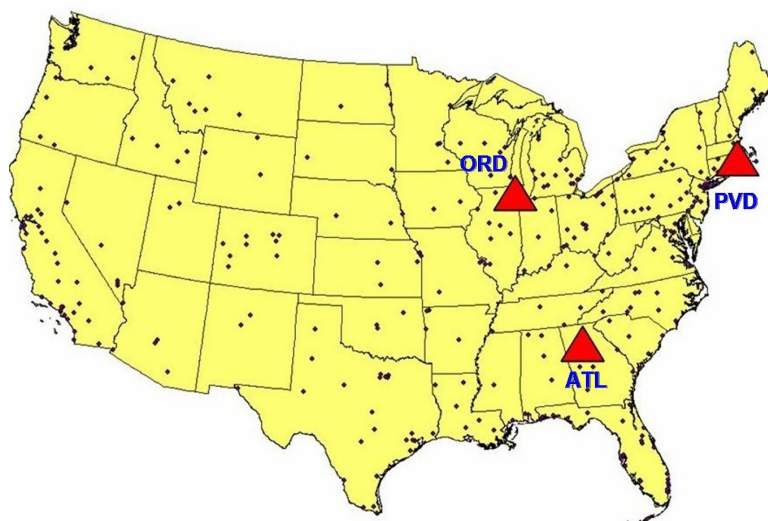
Figure 2.2: Geographic location of 325 airports included in this study. The red triangles represent the three airports (ORD, ATL and PVD) where ambient air quality measurements were made and from which aviation emissions data were generated.

Aviation emissions data from ORD, ATL and PVD were mapped to the other 322 airports located across the contiguous United States (see Appendix A). An airport was mapped with the ground-level aviation emissions from PVD if that airport had the same number or fewer commercial flights (272 airports). Airports with more crossing than parallel runways, or those airports with only parallel runways, were mapped with ground-level aviation emissions from ORD (19 airports). Otherwise, airports were mapped with ground-level aviation emissions from ATL (34 airports). Runway configuration was used to map ground-level aviation emissions because both take-off and landing emissions needed to enter the atmosphere in a similar fashion to maintain consistency with the emission vertical profile. It is important to note that the emissions for nearly 85% of the airports located in the contiguous United States were mapped to PVD, a small regional airport located on the East Coast.

2.2.1 Multiplicative Factor Development

The development of the multiplicative factors has been described in detail elsewhere (Masek, 2008). Multiplicative factors, randomly generated using a Halton low-discrepancy sequence, were applied to simulate increases or decreases in ground-level aviation emissions across the United States due to potential future changes in fleet composition and aviation activities (Masek, 2008). These multiplicative factors were identical for all airports and consequently eliminated any potential regional differences. For example, Los Angeles International Airport (LAX) and John F. Kennedy International Airport (JFK) were both mapped with ground-level aviation emissions from ORD, which did not account for potential meteorological differences due to their location on either coast of the United States. Consequently, ground-level aviation emissions from ORD, ATL and PVD may not best represent conditions in the intermountain west or the Pacific coast. However, the lack of regional specificity does not pose any significant restrictions on the usage of a national model for policy changes (Masek, 2008). Limited amount of actual emissions data and the desire to achieve a baseline understanding of ground-level aviation emissions forced the decision to only use three airports as representations of all other airports in the contiguous United States.

2.2.2 Model Scenarios

Each simulation was designated as "RSM" because these data were used to develop a response surface model (RSM) (Masek, 2008). A base case scenario, designated as RSM999, was representative of current ground-level aviation emissions, to which no multiplicative factors were applied. The other 25 simulation scenarios, representing

increases or decreases in ground-level aviation emissions, were designated RSM001 through RSM025 (Masek, 2008). A multiplicative factor of 1.0 represented current ground-level aviation emissions, while a multiplicative factor greater than 1.0 represented an increase in ground-level aviation emissions. Similarly, a multiplicative factor less than 1.0 represented a decrease in ground-level aviation emissions. The percent increase or decrease in ground-level aviation emissions was determined either by subtracting 1.0 from the multiplicative factor (i.e., increase) or subtracting the multiplicative factor from 1.0 (i.e., decrease). For example, a 342% increase in SO_4^{2-} emissions resulted by subtracting the multiplicative factor of 4.42 from 1.0 (i.e., 4.42 - 1.00 = 3.42, or 342%).

2.3 Human Health Analysis

The primary reason for this study was assessment of human health effects of air quality due to variations in aviation activities. BenMap (Hubbell, 2008) is a GIS-based computer program used by the U.S. EPA to assess the health impacts of pollution change on a given population. BenMap predicts the number of potential future premature deaths (i.e., mortality change) caused by a pollution change (Hubbell, 2008). BenMap also calculates the economic value (i.e., value mortality) associated with the loss of life. Two of the 25 simulations were compared to the base case simulation using BenMap to assess the potential future effects of (a) increases and (b) decreases in total $PM_{2.5}$ concentration on human health.

CHAPTER 3

METHODS

This chapter outlines the methods used to the validate the accuracy of the base case simulation (RSM999), development of the comparative analysis and implementation of BenMap (Hubbell, 2008) for human health effects analysis.

3.1 Validation of the Base Case Simulation

The accuracy of the base case simulation, RSM999, was validated using sampling data from fifty locations within four monitoring networks (Arunachalam *et al.*, 2008). This was accomplished using two different error measurement approaches: the mean fractional error (*MFE*, Eq. 3.1) and the mean fractional bias (*MFB*, Eq. 3.2) (Tonnesen *et al.*, 2005b). The *MFE* is a measure of a simulation's accuracy, comparing predicted values relative to observed values. The *MFB* assesses whether a simulation's predicted values are over or under estimated relative to observed values.

$$MFE = \frac{2}{N} \sum_{i=1}^{n} \left| \frac{P_i - O_i}{P_i + O_i} \right| \tag{3.1}$$

$$MFB = \frac{2}{N} \sum_{i=1}^{n} \left(\frac{P_i - O_i}{P_i + O_i} \right) \tag{3.2}$$

where: P = predicted value, O = observed value.

Performance goals defining three distinct acceptability zones using the *MFE* and *MFB* have been suggested to assess a simulation's predicted values (Boylan & Russell, 2006). These recommendations are based on an analysis of numerous *PM* and visibility modeling studies performed throughout the United States (Boylan & Russell, 2006). The first zone, representing the highest degree of acceptability, is defined as a simulation with *MFE* less than 35% and *MFB* less than 15%. The second zone, representing adequate acceptability, is defined as a simulation with *MFE* less than 50% and *MFB* less than 30%. The third zone, representing questionable a degree of acceptability, is defined as a simulation with *MFE* less than 75% and *MFB* less than 60% (Boylan & Russell, 2006).

3.2   Comparative Analysis

Each of the 25 simulation scenarios was assessed for acceptability using the *MFE* and *MFB*. Randomly selected multiplicative factors were applied to the ground-level aviation emissions causing their variations to occur simultaneously. Two of the three secondary aerosols were held constant to allow assessment of their individual impacts on total $PM_{2.5}$ concentration relative to the base case simulation, RSM999. NO_3^- and NH_4^+ were grouped as semi-volatile *PM* to simplify comparisons.

An increase or decrease in total $PM_{2.5}$ concentration less than 1% between the base case simulation, RSM999, and any of the other 25 simulations, RSM001 through RSM025, was considered negligible with respect to human health effects (Querol *et al.*, 2001). Total $PM_{2.5}$ concentration was determined at each grid cell for the base case simulation and each of the 25 CMAQ simulations. The concentration of each simulation was compared to the corresponding cell of the base case. For each

simulation, a maximum increase or decrease was determined at a specific cell. Because the study area is a geographic or spatial domain, this difference was considered to be the maximum spatial difference. To avoid any negative values for a decrease from the base case, the absolute value of the spatial difference was applied. The change in total $PM_{2.5}$ concentration was defined as the absolute value of the maximum spatial difference between the base case simulation and each of the 25 CMAQ simulations.

To analyze the impact of an individual secondary aerosol, the other two secondary aerosols were considered negligible with respect to human health if the change in total $PM_{2.5}$ concentration was less than 1% from the base case simulation (Querol *et al.*, 2001). If the concentration change of two of the three secondary aerosols was less than 1%, the effects of the third aerosol were directly compared to the base case simulation. Analysis of the 25 simulations resulted in direct comparisons of five simulations outlined in Table 3.1. However, one of the five simulations were not compared directly to RSM999. RSM010 was used as a surrogate base case to analyze the impact of an increase in semi-volatile PM because no direct comparison to semi-volatile PM could be made using RSM999 due to the randomly selected Halton sequence numbers.

Table 3.1: Five simulations whose aviation emissions effect on total $PM_{2.5}$ concentration were compared directly to the base case simulation.

Comparison	Change in Aviation Emissions	Multiplicative Factor
RSM002 to RSM999	63% decrease - SO_4^{2-}	0.37
RSM003 to RSM999	45% increase - SO_4^{2-}	1.45
RSM009 to RSM999	60% increase - OC	1.60
RSM013 to RSM999	342% increase - SO_4^{2-}	4.42
RSM024 to RSM010[a]	176% increase - semi-volatile PM	2.76

[a]RSM010 was used as the base case comparison because no direct comparison to semi-volatile PM could be made using RSM999 due to the randomly selected Halton sequence numbers.

The effects of meteorological forcing functions (i.e., temperature, wind speed, relative humidity) were assessed by comparing winter to summer total $PM_{2.5}$ concentration to determine seasonal variations. February was chosen to represent winter and July represented summer meteorological conditions to allow for the greatest meteorological contrast.

Ten western United States cities were selected for the comparison and included inter-mountain cities (Boise, Idaho; Denver, Colorado; Salt Lake City, Utah), coastal cities (Los Angeles, California; Portland, Oregon; San Diego, California; San Francisco, California; Seattle, Washington) and growing cities (Phoenix, Arizona; Las Vegas, Nevada). Populations estimated for 2000 ranged from 185,787 in Boise, Idaho to 3,694,820 in Los Angeles, California (Bureau, 2008).

3.3 BenMap Health Impacts

The U.S. EPA GIS-based computer program, BenMap (Hubbell, 2008), was used to determine effects of mortality change related to changes in ground-level aviation emissions. A mortality change calculation consists of four separate multiplicative values. The first value is total $PM_{2.5}$ concentration change ($\mu g \ m^{-3}$). The second

value is the mortality effect estimate, which is the change in mortality due to one unit change in ambient air pollution (Hubbell, 2008). The mortality effect estimate used for this study was determined in an epidemiological study conducted by Pope *et al.* (1999). The average change in mortality was approximately 3.7% per $\mu g\ m^{-3}$ change in $PM_{2.5}$ concentration (Pope *et al.*, 1999). The third value is the mortality incidence, which is defined as the average number of deaths in a given population over a period of time (Hubbell, 2008). Approximately 42 deaths in 100,000 occurred due to particulate air pollution exposure PM_{10} in Boise, Idaho (Shprentz, 1996). The fourth value required in determining the mortality change is the size of the exposed population.

The economic value placed on preserving life or eliminating the risk of a premature death is defined as value mortality as calculated with BenMap (Hubbell, 2008). The U.S. EPA analyzed 26 different studies to determine an average value of statistical life (VSL) (Kenkel, 2001). The average VSL was \$6.4 million based on 2001 U.S. dollars. The economic impact on human health associated with exposure to $PM_{2.5}$ calculated by BenMap is the product of mortality change and value mortality and was determined for July 2001 in Boise, Idaho. The economic impact of $PM_{2.5}$ on human health was assessed using changes in SO_4^{2-} ground-level aviation emissions. One simulation represented a 342% increase in SO_4^{2-} ground-level aviation emissions, while the other represented a 63% decrease.

CHAPTER 4

RESULTS AND DISCUSSION

The results of ground-level aviation emissions and their impact on total $PM_{2.5}$ concentration were compared to current emissions. Comparisons were completed that accounted for changes in ground-level aviation emissions and meteorology. The impact on total $PM_{2.5}$ concentration due to changes in each secondary aerosol species is discussed, followed by a discussion of the impact due to varying meteorological effects. Increases and decreases in ground-level aviation emissions were compared. Increases are due to the number of flights, while decreases are due to the potential improvement to engine efficiencies and take-off/landing procedures.

4.1 Base Case Simulation Validation

The *MFE* and *MFB* for the base case simulation, RSM999, were compared to data from four monitoring networks: The Interagency Monitoring of Protected Visual Environments (IMPROVE) (Schichtel, 2008), the Federal Reference Method (FRM) (EPA, 2008a). Speciation Trend Network (STN) (EPA, 2008b) and the U.S. EPA Air Quality System (AQS) (EPA, 2008c). Monitoring data from AQS and IMPROVE monitoring stations were analyzed together because of geographic proximity, as were data for STN and FRM. The results showed that the total $PM_{2.5}$ concentration of the RSM999 simulation produced a *MFB* of less than 20% and a *MFE* of less than 50%; therefore

RSM999 was assumed to be an acceptable simulation (see Section 3.1). This analysis
was performed elsewhere and is described in detail by Arunachalam *et al.* (2008).

4.2   Aviation Emissions Effects

Five comparisons were completed to assess the effect of changes in secondary
aerosols from ground-level aviation emissions on total $PM_{2.5}$ concentration in ten
western United States cities. To fully assess the impact that changes in ground-level
aviation emissions could have on air quality, comparisons examining the effects of
increases and decreases of secondary aerosol species were performed.

4.2.1   Sulfate Emissions Effects

Three comparisons to RSM999 were performed to assess the impact that ground-
level aviation SO_4^{2-} emissions could have on total $PM_{2.5}$ concentration. Ground-
level aviation SO_4^{2-} emissions were increased for both RSM003 (+45%) and RSM013
(+342%) and decreased for RSM002 (-63%) from the base case, RSM999. Figures 4.1
- 4.5 represent the percent change in total $PM_{2.5}$ concentration from the base case
simulation for winter and summer 2001.

The RSM003 simulation represented a 45% increase in SO_4^{2-} emissions from the
base case, RSM999. The maximum increase in total $PM_{2.5}$ concentration during the
winter was 0.15%. Similarly, during the summer, the greatest increase in total $PM_{2.5}$
amongst the ten western cities was 0.09%. Figure 4.1 shows little visible difference in
the percent change of total $PM_{2.5}$ concentration from the base case for both winter
and summer. Because the increase in total $PM_{2.5}$ was less than 1%, a 45% increase in

SO_4^{2-} emissions was considered to have a negligible effect on human health (Querol *et al.*, 2001).

Figure 4.1: Percent change of total $PM_{2.5}$ concentration from the base case (RSM999) due to a 45% increase (RSM003) in ground-level aviation SO_4^{2-} emissions.

The RSM013 simulation represented a 342% increase in ground-level aviation SO_4^{2-} emissions from the base case, RSM999. Los Angeles, California exhibited the greatest percent increase in total $PM_{2.5}$ concentration of 0.18% during the winter. Increases in total $PM_{2.5}$ concentration occurred during the summer for all of the coastal cities. Los Angeles, California (0.40%) and San Francisco, California (0.57%) exhibited increases in total $PM_{2.5}$ concentration. Increases in total $PM_{2.5}$ concentration due to SO_4^{2-} emissions were maximum in and around southern California as illustrated in Figure 4.2. Throughout the study area, the greatest increase in total $PM_{2.5}$ concentration during the winter was only 0.53%. During the summer, the area off the coast of San Diego, California exhibited an increase greater than 1%, indicating that SO_4^{2-} emissions did impact total $PM_{2.5}$ concentration. Ground-level

emissions from any single airport were diluted immediately upon release to the 36 km grid cell in which the airport was located. Because emissions from other sources remained constant, incremental variations in aviation emissions at an individual airport produced only subtle variations in total $PM_{2.5}$ concentration.

Winter   **Summer**
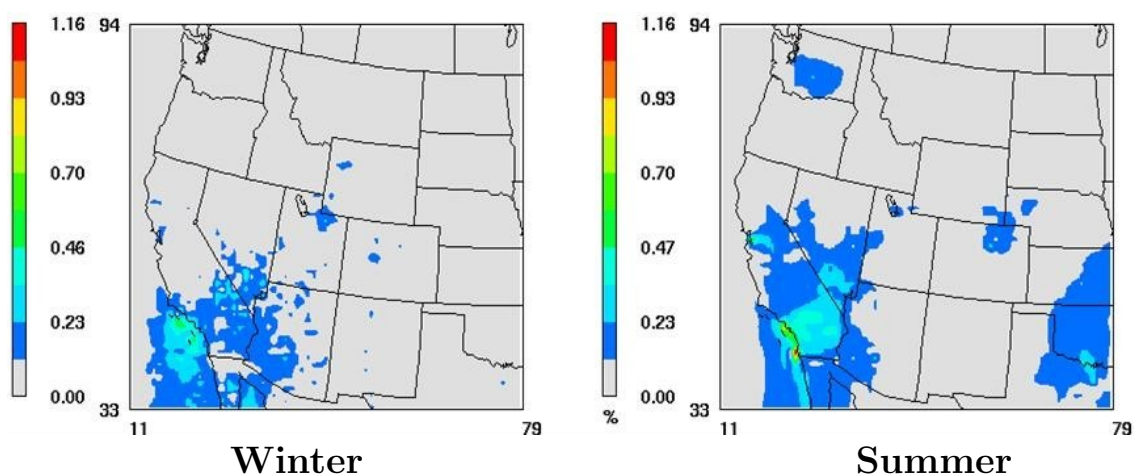
Figure 4.2: Percent change of total $PM_{2.5}$ concentration from the base case (RSM999) due to a 342% increase (RSM013) in ground-level aviation SO_4^{2-} emissions.

The RSM002 simulation represented a 63% decrease in ground-level aviation SO_4^{2-} emissions from the base case, RSM999. Little difference from the base case was observed for each of the ten cities of interest (Figure 4.3). Maximum decreases in total $PM_{2.5}$ concentration for the entire study area (0.39%) were predicted outside Los Angeles and San Diego, California in summer.
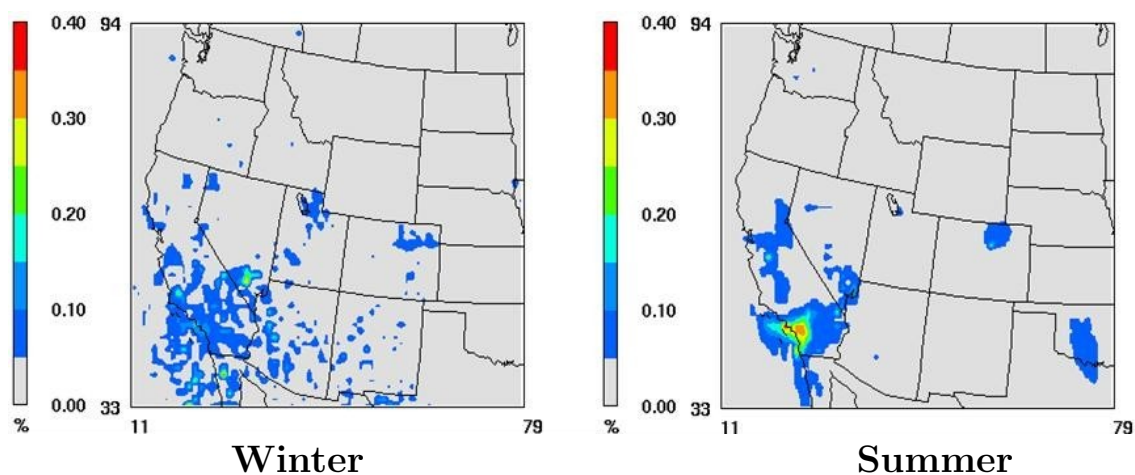
Figure 4.3: Percent change of total $PM_{2.5}$ concentration from the base case (RSM999) due to a 63% decrease (RSM002) in ground-level aviation SO_4^{2-} emissions.

4.2.2 Organic Carbon Emissions Effects

The RSM009 simulation represented a 60% increase in aviation OC emissions from the base case, RSM999. Los Angeles, California exhibited the greatest change in total $PM_{2.5}$ concentration from the base case: 0.089% in the winter and 0.18% during the summer. Figure 4.4 illustrates the locations in the study area that exhibited the maximum increases in total $PM_{2.5}$ concentration during the winter (0.24% near Las Vegas, Nevada) and summer (0.33% in southern California). Because this increase of total $PM_{2.5}$ concentration is less than 1%, the impact to human health is negligible.
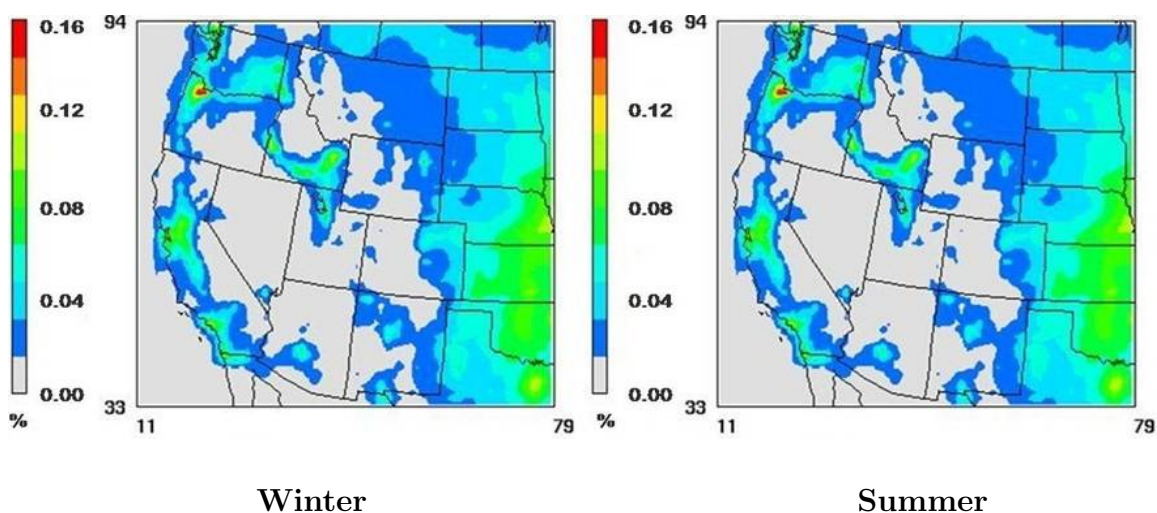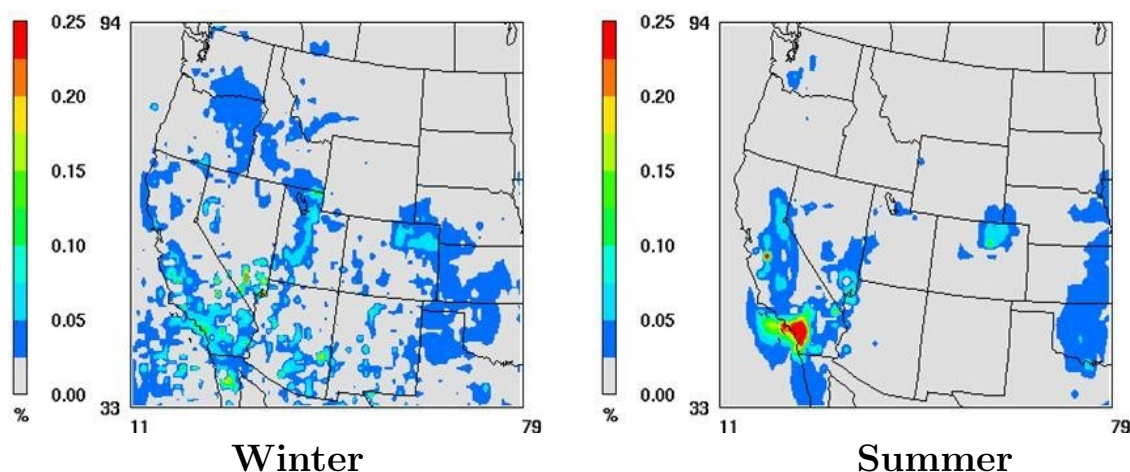
Figure 4.4: Percent change of total $PM_{2.5}$ concentration from the base case due to a 60% increase (RSM009) in ground-level aviation OC emissions.

4.2.3 Semi-volatile PM Emissions Effects

The RSM024 simulation represented a 176% increase in ground-level aviation semi-volatile PM ($NO_3^- + NH_4^+$) emissions from the RSM010 simulation. The RSM010 simulation was used as the surrogate base case, rather than RSM999, because the multiplicative factor applied created a greater difference in semi-volatile PM emissions with RSM024. There was a greater change in total $PM_{2.5}$ concentration in the summer than the winter. Increased change in total $PM_{2.5}$ concentration in summer was more localized around southern California and the San Francisco Bay area (Figure 4.5). There was a 0.46% increase in winter while a 0.60% increase was exhibited in summer. Because this increase of total $PM_{2.5}$ concentration is less than 1%, the impact to human health is negligible.

Winter   **Summer**
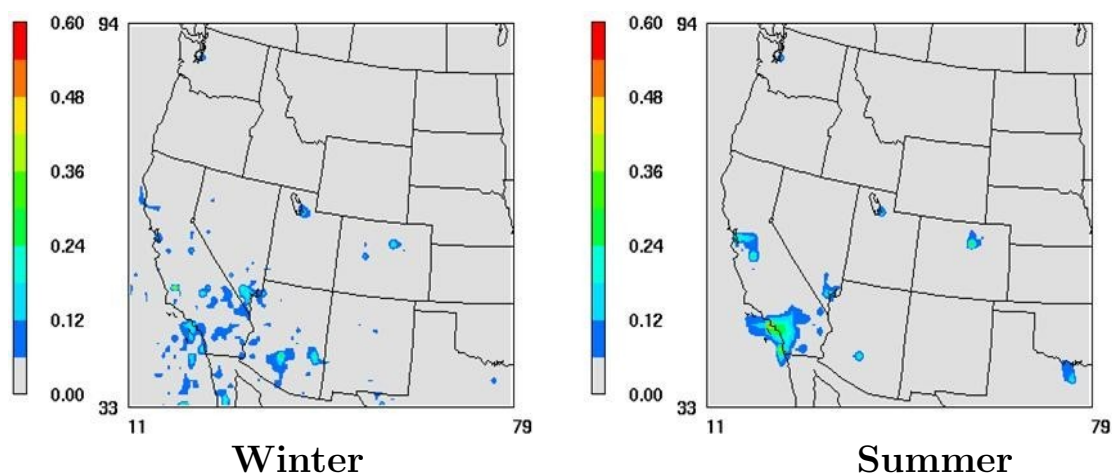
Figure 4.5: Percent change of total $PM_{2.5}$ concentration from the surrogate base case (RSM010) due to a 176% increase (RSM024) in ground-level aviation semi-volatile PM emissions.

4.3 Meteorological Effects

Three meteorological forcing functions and their relationship to total $PM_{2.5}$ concentration are discussed in this section. Temperature, wind speed, and relative humidity effects were analyzed for the base case, RSM999. Temperature is discussed first; followed by wind speed and relative humidity.

4.3.1 Temperature Effects

Temperature data were gathered for each day of February and July, 2001 from the National Climatic Data Center (NCDC) for each of the ten western cities of interest (NCDC, 2008). The average daily temperature was obtained and the arithmetic mean was applied to calculate the monthly average. One study suggested that an increase in temperature would result in an increase of SO_4^{2-} concentration (Dawson *et al.*, 2007). The effects of temperature on SO_4^{2-} concentration are illustrated in Figure 4.6. The difference in SO_4^{2-} concentration between the base case, RSM999,

and the other simulations was greater during the summer for eight of the ten western United States cities. This demonstrates that higher temperatures do contribute to increased SO_4^{2-} concentration. SO_4^{2-} is one of three secondary aerosols considered for this study comprising total $PM_{2.5}$ concentration. Due to the increased temperature, SO_4^{2-} concentration increased, resulting in greater total $PM_{2.5}$ concentration. Average total $PM_{2.5}$ concentration for the ten western cities of interest exhibited an 8.2% increase (0.85 $\mu g\ m^{-3}$ versus 0.93 $\mu g\ m^{-3}$) from summer to winter.
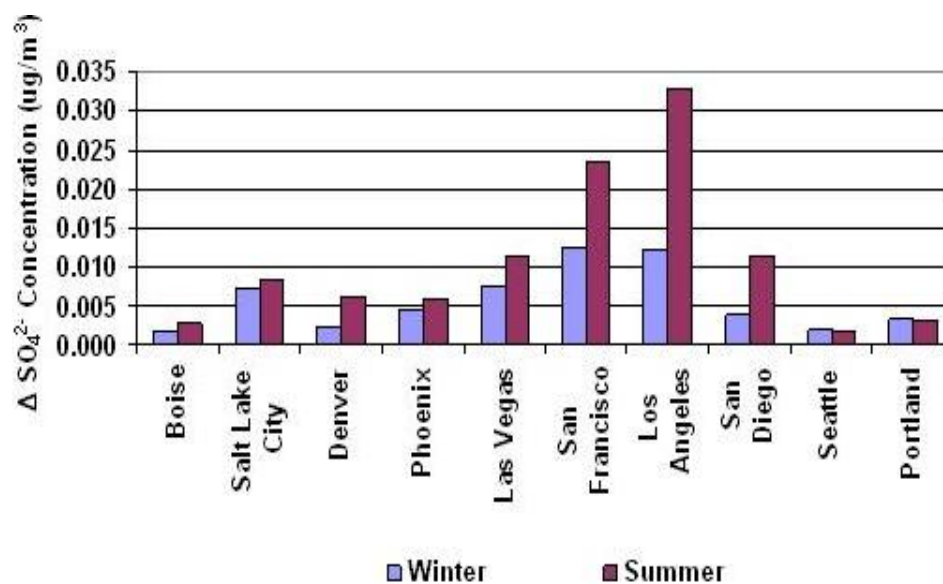
Figure 4.6: Change in aviation SO_4^{2-} concentration from the base case simulation (RSM999) for the winter and summer.

4.3.2 Wind Speed and Directional Effects

Total $PM_{2.5}$ concentrations as a function of average wind speed and direction for the winter and summer are shown in Figure 4.7. Wind directions were classified into 16 zones (22.5 ° increments) that correspond to four cardinal directions. (i.e., north, east, south and west) and 12 intermediate directions (i.e., north northeast, northeast, east

northeast, east southeast, southeast, south southeast, south southwest, southwest, west southwest, west northwest, northwest and north northwest). For example, north was defined as 348.75° to 11.25°; traveling clockwise the next intermediate direction zone was north northeast (11.25° to 33.75°). The average wind direction of the ten western cities of interest was 210° or south southwest.

During the winter, the average wind speed over the study area was 1.9 mph. Only Las Vegas, Nevada and Portland, Oregon exhibited higher wind speeds (3.8 and 4.0 mph, respectively) in the winter. Summertime winds were stronger for coastal cities (6.5 mph for Portland, Oregon and 9.9 mph for San Francisco, California). Conversely, the wind speed for inland cities was low (0.9 mph for Phoenix, Arizona).
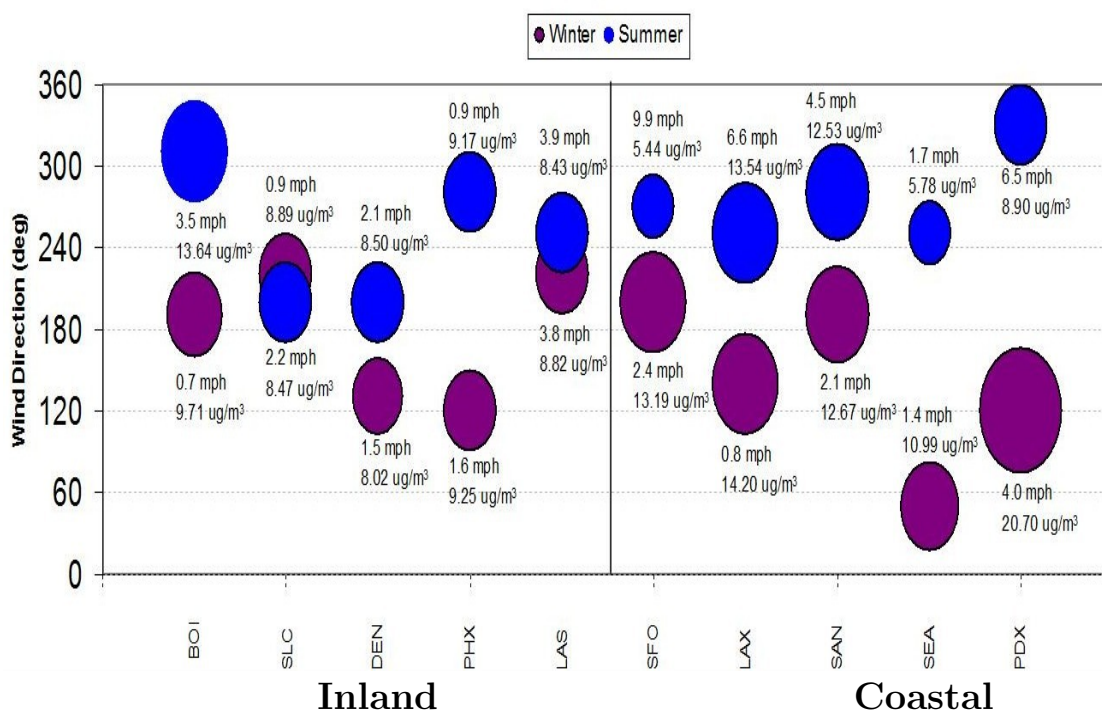
Figure 4.7: Total $PM_{2.5}$ concentrations as a function of average wind speed and direction for ten western United States cities in the winter (purple) and summer (blue) (NCDC, 2008). The size of each bubble is representative of the relative $PM_{2.5}$ concentration associated with each city.

Increased wind speed during the summer caused more advection, which led to decreased total $PM_{2.5}$ concentration along the west coast. Five coastal cities exhibited an average decrease in total $PM_{2.5}$ concentration from 14.3 $\mu g\ m^{-3}$ in the winter to 9.2 $\mu g\ m^{-3}$ in the summer, while the total $PM_{2.5}$ concentration for five inland cities increased from an average of 8.6 $\mu g\ m^{-3}$ to 9.5 $\mu g\ m^{-3}$ during the same time period. There was a 35% decrease along the west coast and a 10% increase inland in total $PM_{2.5}$ concentration during the summer.

4.3.3   Relative Humidity Effects

The effect of relative humidity on total $PM_{2.5}$ formation was investigated for the base case. In the winter, eight of the ten cities exhibited relative humidity greater than 69%. Only desert cities (e.g., Phoenix, Arizona and Las Vegas, Nevada) exhibited relative humidity less than 51%. Inland cities were much drier in the summer with relative humidity averaging 35%, while the coastal cities averaged 75% regardless of season.

Semi-volatile PM concentration was most affected by changes in relative humidity from the winter to summer. The two aerosols that comprise semi-volatile PM, NH_4^+ and NO_3^-, chemically combine within the atmosphere to form ammonium nitrate (NH_4NO_3) (Seinfeld & Pandis, 1998). The effects of relative humidity on the formation of NH_4NO_3 are shown in Figures 4.8 and 4.9.

NH_4NO_3 concentration was higher in the winter because its equilibrium is dependent on temperature and will volatilize with increased temperature during the summer. Also, during the winter, air was more stagnant, creating a more stable atmosphere and subsequent temperature inversions. This allowed NO_3^- and NH_4^+ to accumulate and higher concentrations of NH_4NO_3 to form. More humid air and

limited wind also contributed to the accumulation of NH_4NO_3 during the winter. During the summer, less stagnant air and higher wind speeds caused less accumulation of NH_4NO_3.
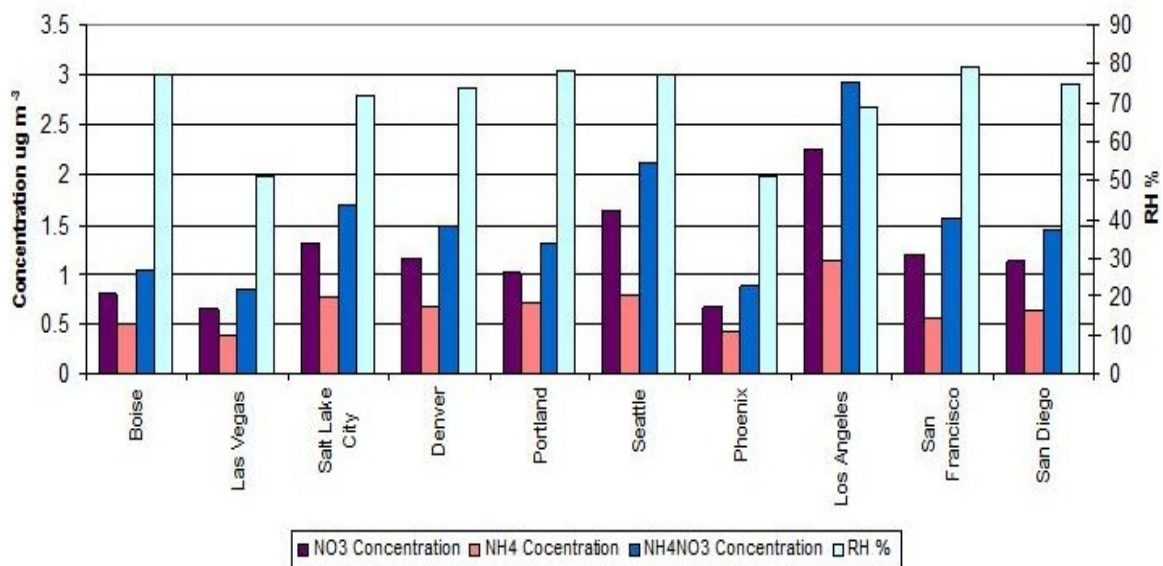
Figure 4.8: Effect of relative humidity on NO_3^-, NH_4^+ and NH_4NO_3 concentrations in the winter.
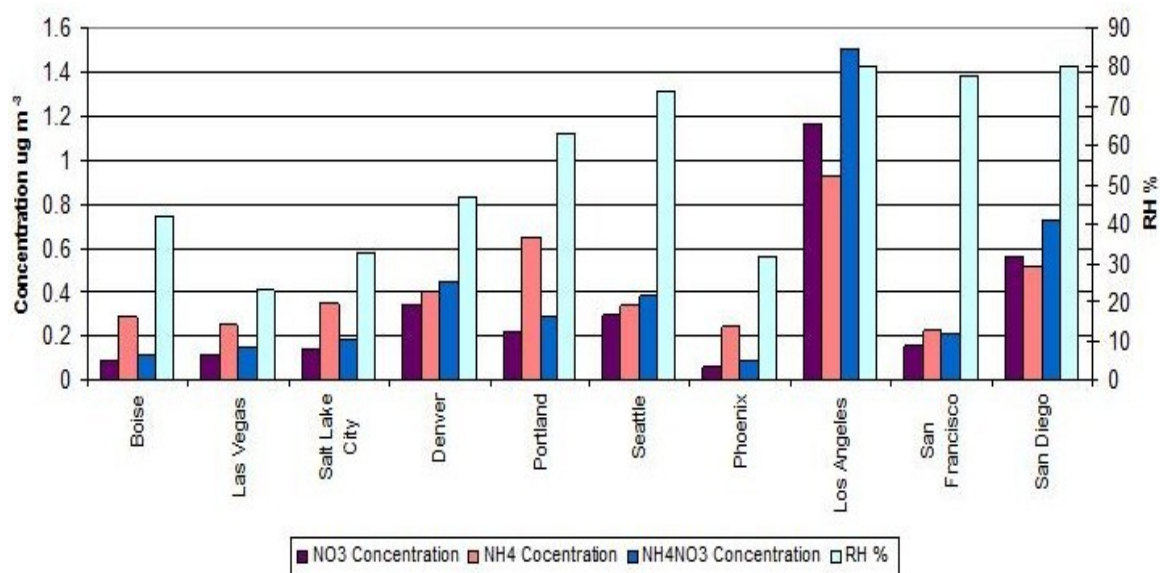
Figure 4.9: Effect of relative humidity on NO_3^-, NH_4^+ and NH_4NO_3 concentrations in the summer.

The higher NH_4NO_3 concentration directly equates to higher concentration of NO_3^- and NH_4^+, the summation of which is semi-volatile PM. Eight of the ten western United States cities exhibited a decrease in relative humidity from winter to summer resulting in lower concentration of NH_4NO_3. Each city with decreased relative humidity exhibited at least an 82% reduction in NH_4NO_3 concentration. Two cities (San Diego and Los Angeles, California) with increased relative humidity in the summer exhibited smaller decreases (approximately 50%) in NH_4NO_3. Higher NH_4NO_3 concentration in the winter (sum of ten cities = 14.55 μg m^{-3}) versus the summer (sum of ten cities = 2.85 μg m^{-3}) indicate NH_4NO_3 concentration was sensitive to relative humidity. A 32.5% decrease in semi-volatile PM ($NO_3^- + NH_4^+$) concentration caused a 18.9% decrease in total $PM_{2.5}$ concentration. The decrease in total $PM_{2.5}$ was due, in large part, to the decrease of in semi-volatile ($NH_4^+ + NO_3^-$) secondary aerosol concentrations, which was due to the decrease of relative humidity.

Figure 4.10 illustrates the change in each secondary aerosol concentration from winter to summer.
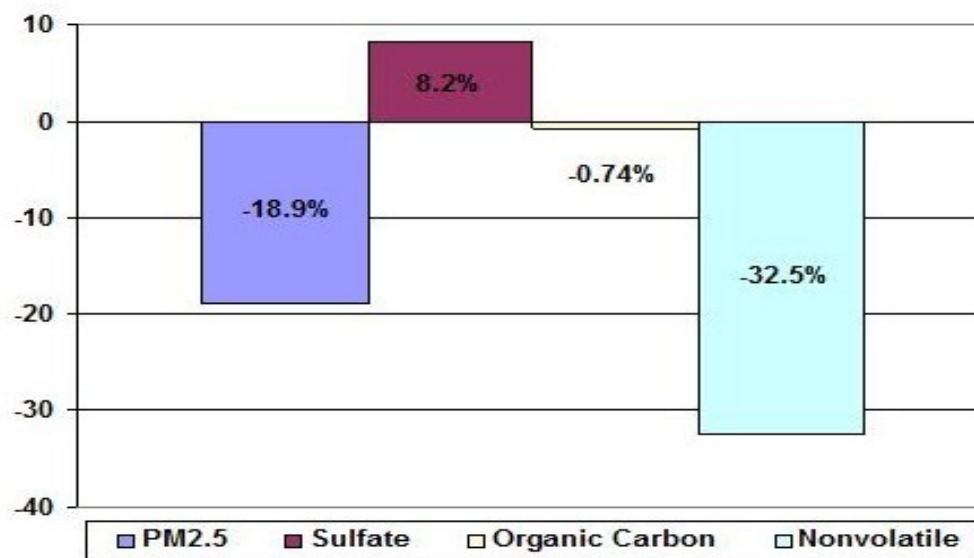
Figure 4.10: Percent change in secondary aerosol concentration from winter to summer.

4.4   Potential Health Effects

Analyses using BenMap (Hubbell, 2008) were performed on two simulations to assess potential health effects in Boise, Idaho. RSM013 represented a 342% increase in ground-level aviation SO_4^{2-} emissions and was selected to examine the impact of a substantial, sustained increase in total $PM_{2.5}$ concentration. RSM002 was chosen to illustrate the economic impact a permanent decrease in ground-level aviation SO_4^{2-} emissions. Summertime meteorological conditions were selected because of the greater change in total $PM_{2.5}$ concentration from the base case, RSM999.

Boise, Idaho exhibited a 0.04 $\mu g\ m^{-3}$ increase in total $PM_{2.5}$ concentration due to a 342% increase in ground-level aviation SO_4^{2-} emissions between the base case and RSM013. The change due to ground-level aviation activities was less than 1.0 $\mu g\ m^{-3}$, which resulted in a mortality effect estimate of 0.015%.

Boise's population was approximately 200,000 in 2001. The mortality incidence (average number of deaths from $PM_{2.5}$ exposure in a given population over a period of time) of 84 annual deaths was assumed to be seven because only one summer month was used in this analysis (Shprentz, 1996). The overall change in mortality (product of concentration change, mortality effect estimate, mortality incidence and affected population) was approximately nine deaths due to an increase in total $PM_{2.5}$ concentration from ground-level aviation activities for one summer month. The monthly cost to eliminate the health risk due to increased total $PM_{2.5}$ concentration was approximately \$533,000 per person based on a \$6.4 million annual value of statistical life (VSL). The economic burden on the community of Boise, Idaho to eliminate the health risk associated with increased ground-level aviation SO_4^{2-} emissions would be \$4.8 million or \$24 per person.

The total $PM_{2.5}$ concentration decrease between RSM999 and RSM002 (63% decrease of ground-level aviation SO_4^{2-} emissions) was only 0.01 $\mu g \ m^{-3}$, which equated to a decrease in SO_4^{2-} exposure mortality by approximately two deaths. The economic burden on the community to reduce the health risk associated with ground-level aviation SO_4^{2-} emissions by 63% and to save two lives from premature death would be approximately \$1.1 to \$1.6 million.

CHAPTER 5

CONCLUSIONS

5.1 Conclusions

Three secondary aerosol components of total $PM_{2.5}$ concentration were analyzed for ten western United States cities. Results indicate that the changes in total $PM_{2.5}$ concentration were driven primarily by meteorology, specifically relative humidity, for cities in the western United States considered in this study. The impacts on total $PM_{2.5}$ concentration due to changes in aviation emissions were small.

An increase in temperature from winter to summer 2001 caused, on average, an 8.2% increase of SO_4^{2-} concentration in urban areas. Semi-volatile PM $(NO_3^- + NH_4^+)$ concentration decreased, on average, 32.5% for the ten cities from the winter to summer because of decreased relative humidity.

Analysis using BenMap (Hubbell, 2008) suggest that approximately nine deaths per month could result from a 342% increase of ground-level aviation SO_4^{2-} emissions in Boise, Idaho. The economic burden on the city to eliminate the associated health risk would be \$4.8 million or \$24 per person. Conversely, BenMap results showed that the maximum cost to decrease ground-level aviation SO_4^{2-} emissions by 63% would be \$8 per person. The BenMap analysis suggests that it is more economically sound, from a health cost perspective, to proactively decrease emissions rather than reactively address the effects of ground-level aviation emissions in the future.

Simulations with CMAQ suggest that ground-level aviation activities do not appear to impact total $PM_{2.5}$ concentration in areas surrounding airports relative to other emission sources (e.g., automobiles, factories). Meteorological factors, specifically relative humidity, tend to cause more fluctuations in total $PM_{2.5}$ concentration than do aviation emissions. However, aviation emissions do have the potential to cause premature deaths if increases are sustained. It is important to continue working towards reducing aviation emissions to keep a minor problem from becoming a major concern.

5.2   Recommendations and Future Research

Because of limited access to aviation emissions data, the ability to generate simulation scenarios limited the situations that could be analyzed. Instead of applying randomly selected multiplicative factors equally, a better approach would be to hold two ground-level aviation emissions at current levels while the third was varied. For example, the effects of SO_4^{2-} emissions could be assessed while OC and semi-volatile PM ($NO_3^- + NH_4^+$) were held constant.

One of the inherent drawbacks of this study was that intermountain west and west coast airports were mapped to airports from the eastern United States. Results suggest that changes in meteorology have greater effect on total $PM_{2.5}$ concentration than do variations in ground-level aviation emissions. Throughout the year, an intermountain western city such as Boise, Idaho has very different meteorological patterns than Chicago, Illinois. The majority (i.e., nearly 85%) of the simulated airports were mapped to a small regional airport in Providence, Rhode Island (PVD) located along the east coast. In the future, there must be wider distribution of

monitored data to better assess the western United States.

Examining only one year of aviation emissions did not provide a true assessment of their effects. Several years of emissions and meteorology data are needed to further develop our understanding of aviation effects on total $PM_{2.5}$ concentration. Meteorology varies from one year to the next; it would be prudent to conduct comparisons with at least five years of data to validate the results.

REFERENCES

Abbey, D., Ostro, B., Petersen, F., & Burchette, R. 1995. Chronic Respiratory Symptoms Associated With Estimated Long-Term Ambient Concentrations of Fine Particulates Less Than 2.5 Microns in Aerodynamic Diameter ($PM_{2.5}$) and Other Air-Pollutants. *Journal of Exposure Analysis and Environmental Epidemiology.*

Arunachalam, S., Baek, B., Wang, B., Davis, N., Holland, A., Adelman, Z., Shanker, U., Binkowski, F., Hanna, A., Thrasher, T., & Soucacos, P. 2008. *An Improved Method to Represent Aviation Emissions in Air Quality Modeling Systems and Their Impact on Air Quality.* Tech. rept. Institute for the Environment, the University of North Carolina, Chapel Hill and CSSI, Inc., Washington D.C.

Binkowski, F. 1999. *Aerosols in Models-3 CMAQ Chapter 10.* Tech. rept. National Exposure Research Laboratory, U.S. Environmental Protection Agency.

Boylan, J., & Russell, A. 2006. PM and Light Extinction Model Performance Metrics, Goals, and Criteria for Three-dimensional Air Quality Models. *Amospheric Environment*, **40**(26), 4946–4959.

Bureau, United States Census. 2008. *2008 Statistics.* http://www.census.gov/.

Chen, T., Shofer, S., Gokhale, J., & Kuschner, W.G. 2007. Outdoor Air Pollution: Overview and Historical Perspective. *The American Journal of the Medical Sciences.*

Ching, J., & Byun, D. 1999. *Introduction to the Models-3 Framework and the Community Multiscale Air Quality Model (CMAQ) Chapter 1.* Tech. rept. National Exposure Research Laboratory, U.S. Environmental Protection Agency.

Dawson, J., Adams, P., & Pandis, S. 2007. Sensitivity of $PM_{2.5}$ to Climate in the Eastern US: A Modeling Case Study. *Atmospheric Chemistry and Physics*, **7**(16), 4295–4309.

DeNavas-Walt, C., Proctor, B., & Lee, C. 2005. *Money Income of Families - Median Income by Race and Hispanic Origin in Current and Constant (2004) Dollars: 1980 to 2004.* Tech. rept. United States Census Bureau, U.S. Statistical Abstract (Table 667).

DOT, US. 2007. *Top 40 Airports in 2004 - Passengers Enplaned: 1994 and 2004.* Tech. rept. United States Census Bureau, U.S. Statistical Abstract (Table 1050).

EPA, US. 2006 (February). *Response Surface Modeling - Technical Support Document for the Proposed PM NAAQS Rule.* Tech. rept. U.S. Environmental Protection Agency: Office of Air Quality Planning and Standards, Research Triangle Park, NC. `http://www.epa.gov/scram001/reports/pmnaaqs_tsd_rsm_all_021606.pdf`.

EPA, US. 2007. *Modeling of the Impact of Aircraft Emissions on Air Quality in Nonattainment Areas (DRAFT)- Technical Support Document EPA 454/R-07-xxx.* Tech. rept. U.S. Environmental Protection Agency: Office of Air Quality Planning and Standards, Research Triangle Park, NC.

EPA, US. 2008a. *Federal Reference Method.* `http://www.bgiusa.com/cau/pm25frm.htm`.

EPA, US. 2008b. *Speciation Trend Network.* `http://www.epa.gov/ttn/airs/airsaqs`.

EPA, US. 2008c. *U.S. EPA Air Quality System.* `http://www.epa.gov/ttn/airs/airsaqs/`.

Gillani, N., & Godowitch, J. 1999. *Plume-In-Grid Treatment of Major Point Source Emissions.* Tech. rept. National Exposure Research Laboratory, U.S. Environmental Protection Agency, Research Triangle Park, North Carolina, EPA 600/R-99/030.

Gryning, S., & Chaumerliac, N. 1997 (June). Air Pollution Modeling and Its Application XII.

Hubbell, B. 2008. *BenMap Environmental Benefits Mapping and Analysis Program User's Manual.* Office of Air Qulity Planning and Standards United States Environmental Protection Agency Research Triangle Park, North Carolina.

ICAO. 2007. *2007 Environmental Report.* Tech. rept. International Civil Aviation Organization. `http://www.icao.int/env/pubs/Env_Report_07.pdf`.

Kenkel, D. 2001. *Using Estimates of the Value of Statistical Life in Regulatory Effects.* Tech. rept. United State Department of Agriculture, Miscellaneous Publication Number 1570.

Masek, T. 2008. *A Response Surface Model of the Air Quality Impacts of Aviation.* Masters of Science, Massachusettes Institute of Technology.

McNally, D. 2003. *Annual Application of MM5 for Calendar Year 2001*. Tech. rept. Apline Geophyics, LLC.

NCDC. 2008. *National Climatic Data Center*. `http://www.ncdc.noaa.gov/oa/ncdc.html`.

Pope, C., Hill, R., & Villegas, G. 1999. Particulate Air Pollution and Daily Mortality on Utah's Wasatch Front. *Environmental Health Perspectives*, **107**(7), 567–573.

Querol, X., Alastuey, A., Rodriguez, S., Plana, F., Ruiz, C., Massague, G., & Puig, O. 2001. PM_{10} and $PM_{2.5}$ Source Apportionment in the Barcelona Metropolitan Area, Catalonia, Spain. *Atmospheric Environment*, **35**(36), 6407–6419.

Schichtel, B. 2008. *The Interagency Monitoring of Protected Visual Environments*. `http://vista.cira.colostate.edu/improve`.

Seinfeld, J., & Pandis, S. 1998. *Atmospheric Chemistry and Physics: From Air Pollution to Climate Change*. Wiley-Science.

Shprentz, D. 1996. *Breath-taking - Premature Mortality Due to Particulate Air Pollution in 239 American Cities 1996*. Tech. rept. Natural Resources Defense Council.

Smallen, D. 2007. *Average Air Fares Reach Highest Fourth-Quarter Level Since 2000; Top 100 Airports: Highest Fare in Anchorage, Lowest Fare at Dallas Love*. Tech. rept. United States Department of Transportation.

Thrasher, T., & Soucacos, P. 2007. *Emissions and Dispersion Modeling System Users Manual*. United States Federal Aviation Administration Office of Environment and Energy and CSSI, Inc. Washington D.C.

Tonnesen, G., Chien, C.J., Omary, M., & Wang, Z. 2005a. *Final Report for the Western Regional Air Partnership (WRAP) Regional Modeling Center (RMC) for the Project Period March 1, 2004, Through February 28, 2005*. Tech. rept. University of California at Riverside.

Tonnesen, G., Wang, B., & Chien, C.J. 2005b. *Quality Model Evaluation Tools v2.0.1 User's Guide: Appendix F of Final WRAP Report 2005*. Air Quality Modeling Group College of Engineering for Environmental Research and Technology University of California Riverside.

UNC. 2008. *Smoke v2.3 User's Manual*. The Institute of the Environment, University of North Carolina at Chapel Hill.

APPENDIX A

AIRPORT DESIGNATION

Listed below are the 325 airports used during this study and the equivalent airport used during the simulations. ATL represents Hartfield/Jackson Atlanta International Airport. ORD is Chicago O'Hare International Airport. And PVD is T.F. Green Regional Airport in Providence, RI.

Table A.1: Airport Designation

Airport Name	City/State	Code	Equiv
Leigh Valley International Airport	Allentown, PA	ABE	PVD
Abilene Regional Airport	Abilene,TX	ABI	PVD
Albuquerque International Sunport	Albuquerque, NM	ABQ	PVD
Southwest Georgia Regional	Albany, GA	ABY	PVD
Nantucket Memorial Airport	Nantucket, MA	ACK	PVD
Atlantic City International Airport	Atlantic City, NJ	ACY	PVD
Addison Airport	Addison, TX	ADS	PVD
Andrews Air Force Base	Camp Springs, MD	ADW	PVD
Alexandria International Airport	Alexandria, LA	AEX	PVD
Fort Worth Alliance	Fort Worth, TX	AFW	PVD
Allegheny County Airport	Pittsburgh, PA	AGC	PVD
Augusta Regional at Bush Field	Augusta, GA	AGS	PVD
Albany International	Albany, NY	ALB	ORD
Rick Husband Amarillo International	Amarillo, TX	AMA	PVD
Ted Stevens International	Anchorage, AK	ANC	ATL
Altoona Blair County Airport	Altoona, PA	AOO	PVD
Centennial Airport	Denver, CO	APA	PVD
Napa County Airport	Napa, CA	APC	PVD
Naples Municipal Airport	Naples, FL	APF	PVD
Aspen-Pitkin Airport	Aspen, CO	ASE	PVD
Hartsfield-Jackson Atlanta International	Atlanta, GA	ATL	ATL
Outagamie County Regional	Appleton, WI	ATW	PVD
Austin-Bergstrom International Airport	Austin, TX	AUS	ATL
Asheville Regional Airport	Fletcher, NC	AVL	PVD
Wilkes-Barre/Scranton International Airport	Scranton, PA	AVP	PVD
Kalamazoo International Airport	Kalamazoo, MI	AZO	PVD
Boca Raton Airport	Boca Raton, FL	BCT	PVD
Bradley International Airport	Windsor Locks, CT	BDL	PVD
Hanscom Field/AFB	Bedford, MA	BED	PVD
King County International Airport	Seattle, WA	BFI	PVD
Meadows Field Airport	Bakersfield, CA	BFL	PVD
Mobile Downtown Airport	Mobile, AL	BFM	PVD
Edwin A Link Field	Binghamton, NY	BGM	PVD
Bangor International Airport	Bangor, ME	BGR	PVD
Hancock County-Bar Harbor Airport	Bar Harbor, ME	BHB	PVD
Birmingham International Airport	Birmingham, AL	BHM	PVD
Billings Logan International Airport	Billings, MT	BIL	PVD
Bismarck Municipal Airport	Bismarck, ND	BIS	PVD
Tulip City Airport	Holland, MI	BIV	PVD
		Continued on next page	

A.1 – Continued from previous page

Airport Name	City/State	Code	Equiv
Rocky Mountain Metropolitan Airport	Broomfield, CO	BJC	PVD
Cleveland Burke Lakefront Airport	Cleveland, OH	BKL	PVD
MidAmerica St. Louis Airport/Scott AFB	Belleville, IL	BLV	PVD
Central Illinois Regional Airport	Bloomington, IL	BMI	PVD
Nashville International Airport	Nashville, TN	BNA	ORD
Boise Airport	Boise, ID	BOI	PVD
Logan International Airport	Boston, MA	BOS	ORD
Southeast Texas Regional Airport	Beaumont, TX	BPT	PVD
Brownsville/South Padre International Airport	Brownsville, TX	BRO	PVD
W.K. Kellogg Regional Airport	Battlecreek, MI	BTL	PVD
Bert Mooney Airport	Butte, MT	BTM	PVD
Baton Rouge Metropolitan Airport	Baton Rouge, LA	BTR	PVD
Buffalo Niagara International Airport	Buffalo, NY	BUF	ORD
Bob Hope Airport	Burbank, CA	BUR	PVD
Baltimore International Airport	Baltimore, MD	BWI	ORD
Gallatin Field Airport	Bozeman, MT	BZN	PVD
Columbia Metropolitan Airport	Columbia, SC	CAE	PVD
Akron-Canton Airport	Akron, OH	CAK	PVD
Cuyahoga County Airport	Cleveland, OH	CGF	PVD
Chattanooga Metropolitan Airport	Chattanooga, TN	CHA	PVD
Charlottesville-Albemarle Airport	Charlottesville, VA	CHO	PVD
Charleston International Airport	Charleston, SC	CHS	PVD
Chico Municipal Airport	Chico, CA	CIC	PVD
The Eastern Iowa Airport	Cedar Rapids, IA	CID	PVD
Cleveland Hopkins International Airport	Cleveland, OH	CLE	ATL
Charlotte Douglas International Airport	Charlotte, NC	CLT	ATL
Port Columbus International Airport	Columbus, OH	CMH	PVD
Univ. of Illinois-Willard Airport	Champaign, IL	CMI	PVD
Colorado Springs Municipal Airport	Colo. Springs, CO	COS	PVD
Natrona County International Airport	Casper, WY	CPR	PVD
St. Louis Downtown Airport	Cahokia, IL	CPS	PVD
Corpus Christi International Airport	Corpus Christi, TX	CRP	PVD
McClellan-Palomar Airport	Carlsbad, CA	CRQ	PVD
Yeager Airport	Charleston, WV	CRW	PVD
Cincinnati/Northern Kentucky International	Hebron, KY	CVG	ATL
Central Wisconsin Airport	Wasau, WI	CWA	PVD
Dayton Beach International Airport	Daytona Beach, FL	DAB	PVD
Dallas Love Field	Dallas, TX	DAL	ATL
James M Cox International Airport	Dayton, OH	DAY	PVD
Ronald Reagan Washington National Airport	Washington, DC	DCA	ORD
Denver International Airport	Denver, CO	DEN	ORD
Coleman A Young International Airport	Detroit, MI	DET	PVD
Dallas-Fort Worth International Airport	Ft Worth TX	DFW	ATL
Duluth Regional Airport	Duluth, MN	DLH	PVD
		Continued on next page	

A.1 – Continued from previous page

Airport Name	City/State	Code	Equiv
DuPage Airport	Chicago, IL	DPA	PVD
Des Moines International Airport	Des Moines, IA	DSM	PVD
Destin-Fort Walton Beach Airport	Destin, FL	DTS	PVD
Detroit Metropolitan Wayne County Airport	Detroit, MI	DTW	ORD
Chippeewa Valley Regional Airport	Eau Claire, WI	EAU	PVD
Ellington Field	Houston, TX	EFD	PVD
Eagle County Regional Airport	Vail/Eagle CO	EGE	PVD
Elmira-Corning Regional Airport	Elmira, NY	ELM	PVD
El Paso International Airport	El Paso, TX	ELP	PVD
Erie International - Tom Ridge Field	Erie, PA	ERI	PVD
Eugene Airport-Mahlon Sweet Field	Eugene, OR	EUG	PVD
Evansville Regional Airport	Evansville, IN	EVV	PVD
Newark Liberty International	Newark, NJ	EWR	ATL
Key West International Airport	Key West, FL	EYW	PVD
Fairbanks International Airport	Fairbanks, AK	FAI	PVD
Hector International Airport	Fargo, ND	FAR	PVD
Fresno Yosemite International Airport	Fresno, CA	FAT	PVD
Fayetteville Regional Airport	Fayetteville, NC	FAY	PVD
Fort Lauderdale International Airport	Ft Lauderdale, FL	FLL	ATL
Bishop International Airport	Flint, MI	FNT	PVD
Republic Airport	Farmingdale, NY	FGR	PVD
Sioux Falls Regional Airport	Sioux Falls, SD	FSD	PVD
Fort Smith Regional Airport	Fort Smith, AR	FSM	PVD
Fort Worth Meacham International Airport	Fort Worth, TX	FTW	PVD
Fulton County Airport	Atlanta, GA	FTY	PVD
Fort Wayne International Airport	Fort Wayne, IN	FWA	PVD
Fort Lauderdale Executive Airport	Fort Lauderdale, FL	FXE	PVD
Spokane International - Geiger Field	Spokane, WA	GEG	PVD
Grand Forks International Airport	Grand Forks, ND	GFK	PVD
Walker Field Airport	Grand Junction, CO	GJT	PVD
Gainesville Regional Airport	Gainesville, FL	GNV	PVD
Groton-New London Airport	New London, CT	GON	PVD
Gulfport-Biloxi International Airport	Gulfport, MS	GPT	PVD
Austin Straubel International Airport	Green Bay, WI	GRB	PVD
Killeen-Fort Hood Regional Airport	Killeen, TX	GRK	PVD
Gerald R Ford International Airport	Grand Rapids, MI	GRR	PVD
Piedmont Triad International Airport	Greensboro, NC	GSO	PVD
Greenville-Spartanburg International Airport	Greenville, SC	GSP	PVD
Great Falls International Airport	Great Falls, MT	GTF	PVD
Manassas Regional Airport-Harry P Davis Field	Manassas, VA	HEF	PVD
Hagerstown Regional Airport	Hagerstown, MD	HGR	PVD
Portland-Hillsboro Airport	Hillsboro, OR	HIO	PVD
Helena Regional Airport	Helena, MT	HLN	ATL
Henderson Executive Airport	Henderson, NV	HND	PVD
		Continued on next page	

A.1 – Continued from previous page

Airport Name	City/State	Code	Equiv
Honolulu International Airport	Honolulu, HI	HNL	ORD
William P Hobby Airport	Houston, TX	HOU	ORD
Westchester County Airport	White Plains, NY	HPN	PVD
Rio Grande Valley International Airport	Harlingen, TX	HRL	PVD
Huntsville International-Carl T Jones Field	Huntsville, AL	HSV	PVD
Tri-State Airport-Milton J Ferguson Field	Huntington, WV	HTS	PVD
Tweed New Haven Regional Airport	New Haven, CT	HVN	PVD
Hilton Head Airport	Hilton Head, SC	HXD	PVD
Barnstable Municipal Airport	Hyannis, MA	HYA	PVD
Washington Dulles International Airport	Washington, DC	IAD	ATL
George Bush Intercontinental Airport	Houston, TX	IAH	ORD
Wichita Mid-Continent Airport	Wichita, KS	ICT	PVD
Idaho Falls Regional Airport-Fanning Field	Idaho Falls, ID	IDA	PVD
Laughlin-Bullhead International Airport	Bullhead City, AZ	IFP	PVD
New Castle Airport	Wilmington, DE	ILG	PVD
Wilmington International Airport	Wilmington, NC	ILM	PVD
Airborne Airpark	Wilmington, OH	ILN	PVD
Indianapolis International Airport	Indianapolis, IN	IND	ATL
Smith Reynolds Airport	Winston-Salem, NC	INT	PVD
Imperial County Airport	Imperial, CA	IPL	PVD
Long Island MacArthur Airport	Islip, NY	ISP	PVD
Ithaca Tompkins Regional Airport	Ithaca, NY	ITH	PVD
Hilo International Airport	Hilo, HI	ITO	PVD
New Century AirCenter	Olathe, KS	IXD	PVD
Inyokern Airport	Inyokern, CA	IYK	PVD
Jackson Hole Airport	Jackson Hole, WY	JAC	PVD
Jackson-Evers International Airport	Jackson, MS	JAN	PVD
Jacksonville International Airport	Jacksonville, FL	JAX	PVD
JFK International Airport	New York, NY	JFK	ORD
Chautauqua County - Jamestown Airport	Jamestown, NY	JHW	PVD
Juneau International Airport	Juneau, AK	JNU	PVD
Concord Regional Airport	Concord, NC	JQF	PVD
John Murtha Johnstown-Cambria County Airport	Johnstown, PA	JST	PVD
Kona International at Keahole	Kona, HI	KOA	PVD
Ketchikan International Airport	Ketchikan, AK	KTN	PVD
Capital City Airport	Lansing, MI	LAN	PVD
McCarran International Airport	Las Vegas, NV	LAS	ORD
Los Angeles International Airport	Los Angeles, CA	LAX	ATL
Lubbock Preston Smith International Airport	Lubbock, TX	LBB	PVD
Arnold Palmer Regional Airport	Latrobe, PA	LBE	PVD
North Platte Regional Airport-Lee Bird Field	North Platte, NE	LBF	PVD
Brazoria County Airport	Lake Johnson, TX	LBX	PVD
Rickenbacker International Airport	Columbus, OH	LCK	PVD
Blue Grass Airport	Lexington, KY	LEX	PVD
		Continued on next page	

A.1 – Continued from previous page

Airport Name	City/State	Code	Equiv
Lafayette Regional Airport	Lafayette, LA	LFT	PVD
LaGuardia Airport	New York, NY	LGA	ORD
Long Beach Municipal Airport	Long Beach, CA	LGB	PVD
Lihue Airport	Kauai Island, HI	LIH	PVD
Little Rock National Airport	Little Rock, AR	LIT	PVD
Klamath Falls Airport	Klamath Falls, OR	LMT	PVD
Lincoln Airport	Lincoln, NE	LNK	PVD
Laredo International Airport	Laredo, TX	LRD	PVD
La Crosse Municipal Airport	La Crosse, WI	LSE	PVD
Lunken Field Municipal Airport	Cincinnati, OH	LUK	PVD
Greenbriar Valley Airport	Greenbriar, WV	LWB	PVD
Gwinnett County Airport	Lawrenceville, GA	LZU	PVD
Midland/Odessa International Airport	Midland/Odessa, TX	MAF	PVD
MBS International Airport	Saginaw, MI	MBS	PVD
Merced Municipal Airport	Merced, CA	MCE	PVD
Kansas City International Airport	Kansas City, MO	MCI	ATL
Middle Georgia Regional Airport	Macon, GA	MCN	PVD
Orlando International Airport	Orlando, FL	MCO	ATL
Harrisburg International Airport	Harrisburg, PA	MDT	PVD
Midway International Airport	Chicago, IL	MDW	ORD
Memphis International Airport	Memphis, TN	MEM	ATL
McAllen-Miller International Airport	McAllen, TX	MFE	PVD
Rouge Valley International Airport	Medford, OR	MFR	PVD
Montgomery International Airport	Montgomery, AL	MGM	PVD
Sacramento Mather Airport	Sacramento, CA	MHR	PVD
Manchester-Boston Regional Airport	Manchester, NH	MHT	PVD
Miami International Airport	Miami, FL	MIA	ATL
Charles B Wheeler Downtown Airport	Kansas City, MO	MKC	PVD
General Mitchell International Airport	Milwaukee, WI	MKE	PVD
Muskegon County Airport	Muskegon, MI	MKG	PVD
Melbourne International Airport	Melbourne, FL	MLB	PVD
Quad City International Airport	Moline, IL	MLI	PVD
Monroe Regional Airport	Monroe, LA	MLU	PVD
Morristown Municipal Airport	Morristown, NJ	MMU	PVD
Mobile Regional Airport	Mobile, AL	MOB	PVD
Modest City-County Airport	Modesto, CA	MOD	PVD
Merrill Field	Anchorage, AK	MRI	PVD
Monterey Peninsula Airport	Monterey, CA	MRY	PVD
Northwest Alabama Regional Airport	Muscle Shoals, AL	MSL	PVD
Dane County Regional Airport	Madison, WI	MSN	PVD
Missoula International Airport	Missoula, MT	MSO	PVD
Minneapolis - Saint Paul International Airport	Minneapolis, MN	MSP	ATL
Louis Armstrong International Airport	New Orleans, LA	MSY	ORD
Montrose Regional Airport	Montrose, CO	MTJ	PVD
		Continued on next page	

A.1 – Continued from previous page

Airport Name	City/State	Code	Equiv
Marthas Vineyard Airport	Marthas Vineyard, MA	MVY	PVD
Myrtle Beach International Airport	Myrtle Beach, SC	MYR	PVD
Naval Air Station - Forrest Sherman Field	Pensacola, FL	NPA	PVD
Oakland International Airport	Oakland, CA	OAK	ATL
Kahului Airport	Kahului, HI	OGG	PVD
Will Rogers World Airport	Oklahoma City, OK	OKC	PVD
Eppley Airfield Airport	Omaha, NE	OMA	PVD
Ontario International Airport	Ontario, CA	ONT	ATL
Opa Locka Airport	Miami, FL	OPF	PVD
O'Hare International Airport	Chicago, IL	ORD	ORD
Norfolk International Airport	Norfolk, VA	ORF	PVD
Orlando Executive Airport	Orlando, FL	ORL	PVD
Ohio State University Airport	Columbus, OH	OSU	PVD
Waterbury-Oxford Airport	Oxford, CT	OXC	PVD
Oxnard Airport	Oxnard, CA	OXR	PVD
Palm Beach International Airport	West Palm Beach, FL	PBI	PVD
Dekalb-Peachtree Airport	Atlanta, GA	PDK	PVD
Portland International Airport	Portland, OR	PDX	ATL
Panama City - Bay County International Airport	Panama City, FL	PFN	PVD
Newport News International Airport	Newport News, VA	PHF	PVD
Philadelphia International Airport	Philadelphia, PA	PHL	ATL
Phoenix Sky Harbor International Airport	Phoenix, AZ	PHX	ATL
Greater Peoria Regional Airport	Peoria, IL	PIA	PVD
St. Petersburg-Clearwater International Airport	St. Petersburg, FL	PIE	PVD
Pocatello Regional Airport	Pocatello, ID	PIH	PVD
Pittsburgh International Airport	Pittsburgh, PA	PIT	ATL
Mid-Ohio Valley Regional Airport	Parkersburg, WV	PKB	PVD
Northeastern Philadelphia Airport	Philadelphia, PA	PNE	PVD
Pensacola Regional Airport	Pensacola, FL	PNS	PVD
Northern Maine Regional Airport	Presque Island, ME	PQI	PVD
Tri-Cities Airport	Pasco, WA	PSC	PVD
Pease International Tradeport Airport	Portsmouth, NH	PSM	PVD
Palm Springs International Airport	Palm Springs, CA	PSP	PVD
Oakland International Airport	Pontiac, MI	PTK	PVD
T.F. Green Regional Airport	Providence, RI	PVD	PVD
Wiley Post Airport	Oklahoma City, OK	PWA	PVD
Chicago Executive Airport	Chicago, IL	PWK	PVD
Portland International Jetport	Portland, ME	PWM	PVD
Rapid City Regional Airport	Rapid City, SD	RAP	PVD
Reading Regional Airport-Carl A. Spaatz Field	Reading, PA	RDG	PVD
Raleigh-Durham International Airport	Raleigh/Durham, NC	RDU	PVD
Chicago/Rockford International Airport	Rockford, IL	RFD	PVD
Richmond International Airport	Richmond, VA	RIC	PVD
Knox County Regional Airport	Rockland, ME	RKD	PVD
		Continued on next page	

A.1 – Continued from previous page

Airport Name	City/State	Code	Equiv
Reno-Tahoe International Airport	Reno, NV	RNO	ATL
Roanoke Regional Airport	Roanoke, VA	ROA	PVD
Greater Rochester International Airport	Rochester, NY	ROC	PVD
Rogers Municipal Airport	Rogers, AR	ROG	PVD
Rochester International Airport	Rochester, MN	RST	ORD
Southwest Florida International Airport	Fort Myers, FL	RSW	PVD
Cobb County Airport	Kennesaw, GA	RYY	PVD
Santa Fe Municipal Airport	Santa Fe, NM	SAF	PVD
San Diego International Airport	San Diego, CA	SAN	ATL
San Antonio International Airport	San Antonio, TX	SAT	PVD
Savannah/Hilton Head International Airport	Savannah, GA	SAV	PVD
Santa Barbara Municipal Airport	Santa Barbara, CA	SBA	PVD
South Bend Regional Airport	South Bend, IN	SBN	PVD
Stockton Metropolitan Airport	Stockton, CA	SCK	PVD
Louisville International Airport-Standiford Field	Louisville, KY	SDF	ATL
Scottsdale Airport	Scottsdale, AZ	SDL	PVD
Seattle-Tacoma International Airport	Seattle, WA Sea-Tac	SEA	ATL
Orlando Sanford International Airport	Orlando, FL Sanford Central	SFB	PVD
San Francisco International Airport	San Francisco, CA	SFO	ORD
Springfield-Branson National Airport	Springfield, MO	SGF	PVD
Sugar Land Regional Airport	Sugar Land, TX	SGR	PVD
Sheridan County Airport	Sheridan, WY	SHR	PVD
Shreveport Regional Airport	Shreveport, LA	SHV	PVD
Sitka Rocky Gutierrez Airport	Sitka, AK	SIT	PVD
San Jose International Airport	San Jose, CA	SJC	ATL
Salt Lake City International Airport	Salt Lake City, UT	SLC	ATL
Salina Municipal Airport	Salina, KS	SLN	PVD
Sacramento International Airport	Sacramento, CA	SMF	PVD
Santa Monica Airport	Santa Monica, CA	SMO	PVD
John Wayne Airport	Santa Ana, CA	SNA	ATL
Abraham Lincoln Capital Airport	Springfield, IL	SPI	PVD
Sarasota-Bradenton International Airport	Sarasota/Bradenton, FL	SRQ	PVD
Lambert-St. Louis International Airport	St. Louis, MO	STL	ATL
St. Paul Downtown Airport - Holman Field	St. Paul, MN	STP	PVD
Friedman Memorial Airport	Sun Valley/Hailey, ID	SUN	PVD
Spirit of Saint Louis Airport	Chesterfield, MO	SUS	PVD
Travis Air Force Base	Fairfield, CA	SUU	PVD
Stewart International Airport	Newburgh, NY	SWF	PVD
Syracuse Hancock International Airport	Syracuse, NY	SYR	PVD
Teterboro Airport	Teterboro, NJ	TEB	PVD
Telluride Regional Airport	Telluride, CO	TEX	PVD
Tallahassee Regional Airport	Tallahassee, FL	TLH	PVD
Tonopah Test Range Airport	Tonopah, NV	TNX	PVD
Toledo Express Airport	Toledo, OH	TOL	PVD
Continued on next page			

A.1 – Continued from previous page

Airport Name	City/State	Code	Equiv
Tampa International Airport	Tampa, FL	TPA	ATL
Tri-Cities Regional Airport	Bristol, TN	TRI	PVD
Trenton-Mercer Airport	Trenton, NJ	TTN	PVD
Tulsa International Airport	Tulsa, OK	TUL	PVD
Tucson International Airport	Tucson, AZ	TUS	PVD
Cherry Capital Airport	Traverse City, MI	TVC	PVD
McGhee Tyson Airport	Knoxville, TN	TYS	PVD
Waukegan Regional Airport	Waukegan, IL	UGN	PVD
University Park Airport	State College, PA	UNV	PVD
Southern California Logistics Airport	Victorville, CA	VCV	PVD
North Las Vegas Airport	Las Vegas, NV	VGT	PVD
Visalia Municipal Airport	Visalia, CA	VIS	PVD
Van Nuys Airport	Van Nuys, CA	VNY	PVD
Okaloosa Regional Airport	Valparaiso, FL	VPS	PVD
McGuire Air Force Base	Wrightstown, NJ	WRI	PVD
Westerly State Airport	Westerly, RI	WST	PVD
Northwest Arkansas Regional Airport	Highfill, AR	XNA	PVD
Willow Run Airport	Detroit, MI	YIP	PVD
Yakima Air Terminal - McAllister Field	Yakima, WA	YKM	PVD
Youngstown-Warren Regional Airport	Youngstown, OH	YNG	PVD
Yuma International Airport	Yuma, AZ	YUM	PVD

APPENDIX B

CMAQ ARCHITECTURE

Table B.1: CMAQ Architecture - This configuration was used for this thesis work when performing the CMAQ simulations.

Component	Version
pfg90 (Fortran Compiler)	7.0.2
NetCDF	3.6.2
ITO PI	3.0
MCI (Meteorology Data)	3.2
CMAQ	4.5